

A Large Manganese-doped Polyoxotitanate Nanocluster: $\text{Ti}_{14}\text{MnO}_{14}(\text{OH})_2(\text{OEt})_{28}$ Yang Chen,^a Jesse Sokolow,^a Elzbieta Trzop,^a Yu-Sheng Chen^b and Philip Coppens^{a,*}^aDepartment of Chemistry, University at Buffalo, State University of New York, Buffalo, New York, 14260-3000, USA^bChemMat CARS, University of Chicago, Chicago, Illinois 60637, USA

(Received: Mar. 30, 2013; Accepted: May 7, 2013; Published Online: May 22, 2013; DOI: 10.1002/jccs.201300163)

A large manganese-doped polyoxotitanate nanocluster, $\text{Ti}_{14}\text{MnO}_{14}(\text{OH})_2(\text{OEt})_{28}$, has been synthesized under solvothermal conditions. Its structure is similar to previously reported $\text{Ti}_{17}\text{O}_{24}(\text{O}^i\text{Pr})_{20}$, but lacks 5-fold coordinated Ti atoms which are potential binding sites for photosensitizer molecules. The Mn atom is located at the center of the Keggin structure with Ti-O bond length indicative of Mn^{2+} , a conclusion confirmed by NEXAFS measurements. Solid-state band gap measurements of the complex show a significant decrease compared with undoped polyoxotitanate nanoclusters and anatase, indicating the potential of Mn-doping for visible light photocatalysis.

Keywords: Transition metal doping; Polyoxotitanate; Nanocluster; Crystal structure; Band gap.

INTRODUCTION

During the past decades, titanium dioxide (TiO_2) has been extensively investigated because of its capacity for photocatalytic degradation of organic pollutants in water or air as a result of the photo-induced generation of electron-hole pairs.¹ In particular the anatase polymorph has been widely used as a photocatalyst. However, because of its relatively large band gap of ~ 3.2 eV its photo-activity is limited to exposures by ultraviolet (UV) light.^{2,3} To reduce the band gap attention has focused on modifying the energy levels by doping.⁴⁻⁷ In 2002, K. Asai *et al.* reported a theoretical calculation of an assembly of rutile unit cells doped with 3d transition metals (3dTM) (V, Cr, Mn, Fe, Co and Ni) and showed that the band gap was significantly affected.⁵ The calculations indicated that as the atomic number of the 3dTM dopant increases, localized levels of the dopant atoms shift to lower energies, and enter the band gap in the case of Cr, Mn and Fe. To provide experimental support we have continued our earlier work on polyoxotitanate nanoclusters^{3,8-10} by synthesizing nanoclusters doped with Mn. We report here the synthesis, structure and properties of the nanocluster $\text{Ti}_{14}\text{MnO}_{14}(\text{OH})_2(\text{OEt})_{28}$, which is the largest Ti/Mn polyoxotitanate reported so far.⁶

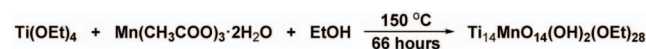
EXPERIMENTAL

Synthesis. All chemicals and solvent were obtained from commercial sources and used as received: Titanium(IV) ethoxide (99+ %) was purchased from Alfa Aesar; manganese(III) acetate dihydrate (97%) from Aldrich Chem. Co.; and ethanol (200 proof,

anhydrous, $\geq 99.5\%$) from SIGMA-ALDRICH. All compounds containing titanium were stored and handled in a glove-box under a nitrogen atmosphere.

Synthesis of $\text{Ti}_{14}\text{MnO}_{14}(\text{OH})_2(\text{OEt})_{28}$: To a Teflon-lined Parr bomb with a capacity of 23 mL were added titanium(IV) ethoxide (1.09 g, 4.77 mmol), manganese(III) acetate dihydrate (0.07 g, 0.25 mmol) and ethanol (5.0 mL) in a glove-box. After the mixture was stirred for about 5 minutes, the bomb was sealed, then placed in a 150 °C oven for 66 hours. Subsequent cooling to room temperature yielded pale-yellow block crystals of $\text{Ti}_{14}\text{MnO}_{14}(\text{OH})_2(\text{OEt})_{28}$. They were collected by filtration, washed with ethanol and dried in the glove-box. Yield: 22.7 mg (4.0% based on Mn). The overall reaction is summarized in Scheme I.

Scheme I Reaction on synthesis of $\text{Ti}_{14}\text{MnO}_{14}(\text{OH})_2(\text{OEt})_{28}$ under solvothermal conditions



Characterization of the product

Energy Dispersive Spectroscopy. The EDS (energy-dispersive X-ray spectroscopy) spectrum of $\text{Ti}_{14}\text{MnO}_{14}(\text{OH})_2(\text{OEt})_{28}$ is shown in Fig. 1. The resulting atomic ratio of Ti:Mn is found as 14.38:1, which, given the large relative uncertainty of 25% (1σ , see the text in Fig. 1) in the Mn content, agrees within the experimental uncertainty with the value 14:1 ratio from the crystal structure. The EDS result is in agreement with the observed MnO bond length as discussed in the next section.

Special Issue Dedicated to Prof. Yu Wang in Honor of Her 70th Birthday

* Corresponding author. E-mail: coppens@buffalo.edu

X-Ray Crystallography. Data on $\text{Ti}_{14}\text{MnO}_{14}(\text{OH})_2(\text{OEt})_{28}$ were collected on a $0.18 \times 0.19 \times 0.26$ mm crystal at 90 K on a Bruker SMART APEXII CCD diffractometer with a Bruker TXS microfocus rotating anode ($\text{MoK}\alpha$ radiation, $\lambda = 0.71073$ Å), equipped with Helios Optics and an Oxford Cryosystems nitrogen flow apparatus. Data integration down to 0.82 Å resolution was carried out using *SAINTE* V7.68¹¹ with reflection spot size optimization. Absorption corrections were made with the program *SADABS*. The structure was solved by direct methods and refined by least-squares against F^2 using *SHELXS-97* and *SHELXL-97*.¹² Non-hydrogen atoms were refined anisotropically. All hydrogen atoms were placed in geometrically idealized positions and constrained to ride on their parent atoms. Analysis of the data program *PLATON*^{13,14} indicated the presence of merohedral twinning. The resulting twin law (0 1 0 / 1 0 0 / 0 0 -1) was applied with the TWIN/BASF combination of *SHELX*. The twin ratio corresponded to 28.86(5)% contribution of the minor twin component. Crystal data as well as details of data collection and refinement of the structure are listed in Table 1. Full details can be found in CCDC-930833, which can be obtained free of charge via <http://www.ccdc.cam.ac.uk/conts/retrieving.html> or deposit@ccdc.cam.ac.uk (the Cambridge Crystallographic Data Center, 12 Union Road, Cambridge CB2 1EZ, UK; Fax: (+44) 1223-336-033).

X-ray absorption spectroscopy. XANES spectra at the Mn absorption edge were collected at beamline 15-ID at the Advanced Photon Source (APS). The result indicate that the absorption edge is below the monochromator limit of 6.2 keV for both the title complex and the reference compound MnBr_2 , compared with a value of 6.542 keV for $\text{Mn}(\text{acetate})_3$. The assignment of the Mn^{2+} valence is in agreement with the crystallographically determined M-O bond lengths, as discussed in the following section.

RESULTS AND DISCUSSIONS

Crystal structure

$\text{Ti}_{14}\text{MnO}_{14}(\text{OH})_2(\text{OEt})_{28}$ crystallizes in the tetragonal space group $I\bar{4}$. The crystal structure is shown in Fig. 2a.

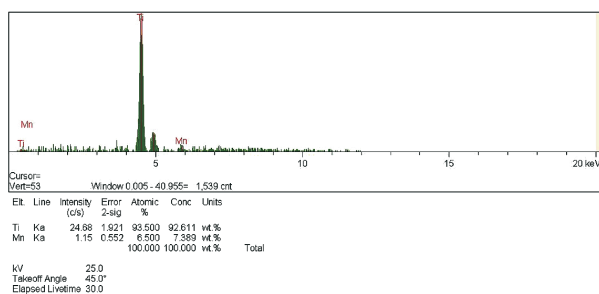


Fig. 1. EDS spectrum of $\text{Ti}_{14}\text{MnO}_{14}(\text{OH})_2(\text{OEt})_{28}$.

Table 1. Crystal data and structure refinement of $\text{Ti}_{14}\text{MnO}_{14}(\text{OH})_2(\text{OEt})_{28}$

Compound	$\text{Ti}_{14}\text{MnO}_{14}(\text{OH})_2(\text{OEt})_{28}$
Crystal	pale-yellow block
Crystal system	Tetragonal
Space group	$I\bar{4}$
a (Å)	14.0240(6)
b (Å)	14.0240(6)
c (Å)	23.8386(11)
V (Å ³)	4688.4(4)
Z	2
Density (g cm ⁻³)	1.589
μ ($\text{MoK}\alpha$) (mm ⁻¹)	1.332
$F(000)$	2322
θ range (°)	1.71 ~ 28.31
Reflections collected	46261
Independent reflections	5850
$R1$ (%) ($I > 2\sigma(I)$)	1.65
$\omega R2$ (%) ($I > 2\sigma(I)$)	4.54
$R1$ (%) (All data)	1.67
$\omega R2$ (%) (All data)	4.56
S	1.028
$\Delta\rho_{\text{max}} / \Delta\rho_{\text{min}}$ (e Å ⁻³)	0.232 / -0.192

The complex is located on the 4-fold inversion center with $1/4$ of the molecule in the asymmetric unit. The $\text{Ti}_{14}\text{MnO}_{44}$ core is similar to the $\text{Ti}_{17}\text{O}_{44}$ core of the $\text{Ti}_{17}\text{O}_{24}(\text{O}^i\text{Pr})_{20}$ cluster,^{3,15} except that two of the five-coordinated Ti atoms are missing and one Ti is replaced by Mn, whereas the other five-coordinated Ti atoms of $\text{Ti}_{14}\text{MnO}_{14}(\text{OH})_2(\text{OEt})_{28}$ are octahedrally coordinated (Fig. 3b). The Mn atom is tetrahedrally coordinated to four oxygen atoms, with a single unique Mn-O bond length of 2.057(2) Å, which is typical for Mn^{2+} , as is the tetrahedral coordination for a d^5 transi-

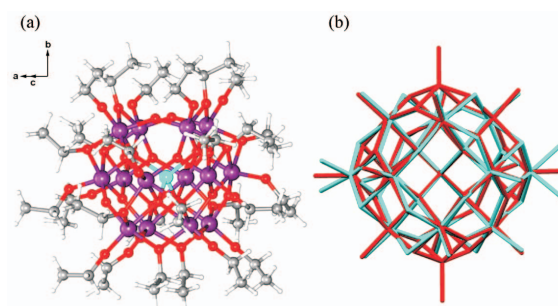


Fig. 2. (a) Perspective view of the $\text{Ti}_{14}\text{MnO}_{14}(\text{OH})_2(\text{OEt})_{28}$ cluster. Atom color codes: Ti, purple; Mn, cyan; O, red; C, grey; H, light grey. (b) Structural overlay of the $\text{Ti}_{14}\text{MnO}_{44}$ core in $\text{Ti}_{14}\text{MnO}_{15}(\text{OH})(\text{OEt})_{28}$ and the $\text{Ti}_{17}\text{O}_{44}$ core in $\text{Ti}_{17}\text{O}_{24}(\text{O}^i\text{Pr})_{20}$. $\text{Ti}_{14}\text{MnO}_{44}$, cyan; $\text{Ti}_{17}\text{O}_{44}$, red.

Table 2. Average Mn-O distance for different Mn valencies¹⁷

Valency	Average distance (Å)
Mn ²⁺	2.100
Mn ³⁺	1.915
Mn ⁴⁺	1.915
Mn ⁷⁺	1.588

tion metal atom.¹⁶

Spectroscopy

Optical diffuse-reflection spectra of the crystalline solids Ti₁₄MnO₁₄(OH)₂(OEt)₂₈ and commercial anatase TiO₂ were measured at room temperature. The absorption (α/S) data were calculated from the reflectance using the Kubelka–Munk function.¹⁸ The resulting energy band gaps (E_{onset}) obtained by extrapolation of the linear portion of the absorption edges are 2.64 eV for Ti₁₄MnO₁₄(OH)₂(OEt)₂₈ (Fig. 4a) and 3.19 eV for anatase (Fig. 4b). It is noticeable that the value of energy band gap of the doped cluster Ti₁₄MnO₁₄(OH)₂(OEt)₂₈ is red-shifted 0.55 eV with respect to that of commercial anatase and smaller than that of the undoped Ti17 nanoparticle.³

Band Structure Calculation

The band structure of the complex (Fig. 5) was calcu-

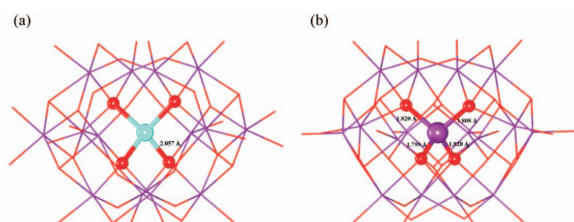


Fig. 3. (a) The Ti₁₄Mn oxocluster in Ti₁₄MnO₁₄(OH)₂(OEt)₂₈. The Mn-O bond length is indicated. (b) The Ti₁₇O₄₄ core of Ti₁₇O₂₄(OⁱPr)₂₀ with the Ti_{center}-O bond distances.

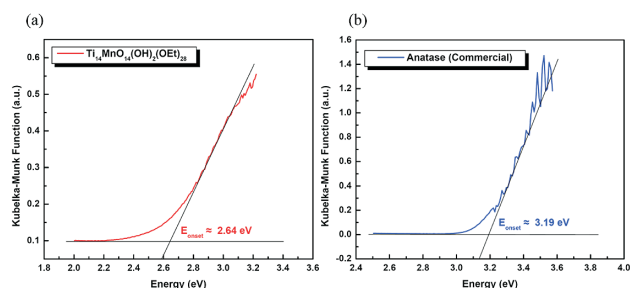


Fig. 4. Solid state optical diffuse-reflection spectra of Ti₁₄MnO₁₄(OH)₂(OEt)₂₈ and commercial anatase derived from diffuse reflectance data (room temperature).

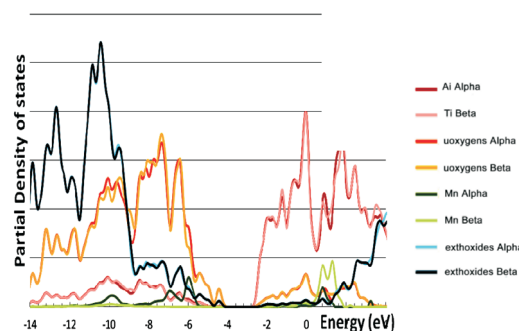


Fig. 5. Calculated band structure of Ti₁₄MnO₁₄(OH)₂(OEt)₂₈.

lated with Gaussian09¹⁹ using the B3LYP functional²⁰ and 6-31G basis sets.²¹ Mn²⁺ has been treated as a sextet high-spin configuration in the calculation.²² The resulting α - and β -orbital density of states are depicted in the figure. Compared with the calculated band gaps of other small polyoxotitanate clusters³ and of anatase the band gap is significantly reduced by the manganese doping, in agreement with the spectroscopic measurements discussed above. The most likely transition corresponding to the 2.64 eV value observed spectroscopically is from the oxygen orbitals in the valence band to the lowest Ti orbitals in the conduction band which are separated by ~ 2.5 eV in the band structure diagram.

CONCLUSIONS

We conclude that doping of the Ti/O nanoparticle with manganese leads to a significant reduction of the band gap, indicating the potential of Mn doping to increase the use of visible light in photocatalysis by semiconductor nanoparticles. The current study is part of a larger project to synthesize bare and sensitized polyoxotitanate nanoparticles and investigate their structures and photo-physical properties.^{3,8-10}

ACKNOWLEDGEMENTS

We thank Peter J. Bush, Director of the South Campus Instrument Center, for assistance with the EDS spectrum analysis. This work was funded by the Division of Chemical Sciences, Geosciences, and Biosciences, Office of Basic Energy Sciences of the U.S. Department of Energy through Grant DE-FG02-02ER15372. ChemMatCars (Sector 15) is principally supported by the National Science Foundation/Department of Energy under Grant CHE-0822838. Use of the APS was supported by the U.S. De-

partment of Energy, Office of Science, Office of Basic Energy Sciences, under Contract DE-AC02-06CH11357.

REFERENCES

1. Linsebigler, A. L.; Lu, G.; Yates, J. T. *Chem. Rev.* **1995**, *95*, 735.
2. Valencia, S.; Marín, J. M.; Restrepo, G. *Open Mater. Sci. J.* **2010**, *4*, 9.
3. Benedict, J. B.; Coppens, P. *J. Am. Chem. Soc.* **2010**, *132*, 2938.
4. Zaleska, A. *Recent Pat. Eng.* **2008**, *2*, 157.
5. Iwasaki, M.; Hara, M.; Kawada, H.; Tada, H.; Ito, S. *J. Colloid Interface Sci.* **2000**, *224*, 202.
6. In, S.; Orlov, A.; Garcia, F.; Tikhov, M.; Wright, D. S.; Lambert, R. M. *Chem. Commun.* **2006**, 4236.
7. In, S.; Orlov, A.; Berg, R.; Garcia, F.; Pedrosa-Jimenez, S.; Tikhov, M. S.; Wright, D. S.; Lambert, R. M. *J. Am. Chem. Soc.* **2007**, *129*, 13790.
8. Benedict, J. B.; Freindorf, R.; Trzop, E.; Cogswell, J.; Coppens, P. *J. Am. Chem. Soc.* **2010**, *132*, 13669.
9. Snoberger III, R. C.; Young, K. J.; Tang, J.; Allen, L. J.; Crabtree, R. H.; Brudvig, G. W.; Coppens, P.; Batista, V. S.; Benedict, J. B. *J. Am. Chem. Soc.* **2012**, *134*, 8911.
10. Sokolow, J. D.; Trzop, E.; Chen, Y.; Tang, J.; Allen, L. J.; Crabtree, R. H.; Benedict, J. B.; Coppens, P. *J. Am. Chem. Soc.* **2012**, *134*, 11695.
11. Bruker AXS: Madison, WI, 1999.
12. Sheldrick, G. M. *Acta Crystallogr., A* **2008**, *64*, 112.
13. Spek, A. L. *J. Appl. Cryst.* **2003**, *36*, 7.
14. Spek, A. L. *Acta Crystallogr. Sect. D-Biol. Crystallogr.* **2009**, *65*, 148.
15. Steunou, N.; Kickelbick, G.; Boubekeur, K.; Sanchez, C. M. *J. Chem. Soc., Dalton Trans.* **1999**, 3653.
16. Crabtree, R. H. *The Organometallic Chemistry of the Transition Metals*, 4th ed.; John Wiley: Hoboken, N.J., 2005.
17. Wilson, A. J. C.; Prince, E. *International Tables for Crystallography. Volume C, Mathematical, Physical, and Chemical Tables*, 2nd ed.; Published for the International Union of Crystallography by Kluwer Academic Publishers: Dordrecht, 1999.
18. Wendlandt, W. W.; Hecht, H. G. *Reflectance Spectroscopy*; Interscience Publishers: New York, 1966.
19. Frisch, M. J.; Trucks, G. W.; Schlegel, H. B.; Scuseria, G. E.; Robb, M. A.; Cheeseman, J. R.; Scalmani, G.; Barone, V.; Mennucci, B.; Petersson, G. A.; Nakatsuji, H.; Caricato, M.; Li, X.; Hratchian, H. P.; Izmaylov, A. F.; Bloino, J.; Zheng, G.; Sonnenberg, J. L.; Hada, M.; Ehara, M.; Toyota, K.; Fukuda, R.; Hasegawa, J.; Ishida, M.; Nakajima, T.; Honda, Y.; Kitao, O.; Nakai, H.; Vreven, T.; Montgomery, J., J. A.; Peralta, J. E.; Ogliaro, F.; Bearpark, M.; Heyd, J. J.; Brothers, E.; Kudin, K. N.; Staroverov, V. N.; Kobayashi, R.; Normand, J.; Raghavachari, K.; Rendell, A.; Burant, J. C.; Iyengar, S. S.; Tomasi, J.; Cossi, M.; Rega, N.; Millam, J. M.; Klene, M.; Knox, J. E.; Cross, J. B.; Bakken, V.; Adamo, C.; Jaramillo, J.; Gomperts, R.; Stratmann, R. E.; Yazyev, O.; Austin, A. J.; Cammi, R.; Pomelli, C.; Ochterski, J. W.; Martin, R. L.; Morokuma, K.; Zakrzewski, V. G.; Voth, G. A.; Salvador, P.; Dannenberg, J. J.; Dapprich, S.; Daniels, A. D.; Farkas, Ö.; Foresman, J. B.; Ortiz, J. V.; Cioslowski, J.; Fox, D. J.; Gaussian, I., Ed. Wallingford, CT, 2009.
20. Becke, A. D. *J. Chem. Phys.* **1988**, *88*, 2547.
21. Krishnan, R.; Binkley, J. S.; Seeger, R.; Pople, J. A. *J. Chem. Phys.* **1980**, *72*, 650.
22. Cotton, F. A.; Wilkinson, G. *Advanced Inorganic Chemistry: A Comprehensive Text*, 4th ed.; Wiley: New York, 1980.